Translational Oncology
www.transonc.com

Volume 6 Number 1 February 2013 pp. 33–41 33

High-Resolution Optical Molecular Imaging of Changes in Choline Metabolism in Oral Neoplasia[1]

Zhen Luo*[,2], Melissa Loja[†,2], D. Greg Farwell[‡], Quang C. Luu[‡], Paul J. Donald[‡], Deborah Amott[‡], Regina Gandour-Edwards[§] and Nitin Nitin*[,¶]

*Department of Biological and Agricultural Engineering, University of California, Davis, Davis, CA; [†]School of Medicine, University of California, Davis, Davis, CA; [‡]Department of Otolaryngology, University of California, Davis, Davis, CA; [§]Department of Pathology and Laboratory Medicine, University of California, Davis, Davis, CA; [¶]Food Science and Technology, University of California, Davis, Davis, CA

Abstract

This study was aimed at developing an optical molecular imaging approach to measure differences in uptake and intracellular retention of choline in clinically isolated tissue biopsies from head and neck cancer patients. An optically detectable analogue of choline (propargyl choline) was synthesized and evaluated in 2D and 3D models and clinically isolated paired biopsies ($n = 22$ biopsies). Fluorescence contrast between clinically abnormal and normal tissues based on uptake and intracellular retention of propargyl choline was measured and correlated with pathologic diagnosis. Results in 2D and 3D models demonstrated a rapid uptake of propargyl choline in cancer cells, uniform permeation in tissue models, and specific detection of intracellular entrapped propargyl choline using the click chemistry reaction with an azide-modified Alexa 488 dye. Fluorescence imaging measurements following topical delivery of propargyl choline in clinically isolated biopsies showed that the mean fluorescence intensity (MFI) of neoplastic tissues was four-fold to five-fold higher than the MFI of clinically and pathologically normal samples. This difference in fluorescence contrast was measured on the basis of comparison of paired biopsy sets isolated from individual patients as well as comparison of clinically abnormal and normal biopsies independent of anatomic locations in the head and neck cavity and across diverse patients. In conclusion, a novel imaging approach based on monoalkyne-modified choline was developed and validated using cell and tissue models. Results in clinically isolated tissue biopsies demonstrate a significant fluorescent contrast between neoplastic and normal tissues and illustrate high specificity of the optical imaging approach.

Translational Oncology (2013) 6, 33–41

Introduction

Optical molecular imaging technology has significant potential to improve early detection and prognostic assessment of cancer [1–3]. Advances in biophotonic instrumentation have enabled both high-resolution and wide-field imaging of tissues in both laboratory and clinical environment [4–7]. To develop molecular-specific optical imaging approaches, we have developed a large diversity of molecular probes such as molecular beacon–based activatable probes and nanoparticle-based contrast agents [8–10].

Despite these significant developments, there are only limited numbers of translational studies focused on evaluating these optical molecular

Address all correspondence to: Nitin Nitin, PhD, Department of Biological Engineering, University of California, Davis, One Shields Avenue, Davis, CA 95616. E-mail: nnitin@ucdavis.edu

[1]This project was supported by the National Center for Research Resources (NCRR), National Institutes of Health (NIH) through grant UL1 RR024146 and linked award TL1 RR024145. Its contents are solely the responsibility of the authors and do not necessarily represent the official view of NCRR or NIH. Information on Re-engineering the Clinical Research Enterprise can be obtained from http://nihroadmap.nih.gov/clinicalresearch/overview-translational.asp. Authors declare no conflicts of interest.
[2]Both authors contributed equally to this work.
Received 24 August 2012; Revised 14 December 2012; Accepted 18 December 2012

DOI 10.1593/tlo.12289

imaging probes in clinical samples [11–15]. In a clinical environment, positron emission tomography (PET) imaging is the leading molecular imaging approach. Many of the clinical PET imaging methods are based on uptake of radiolabeled small metabolites such as deoxyglucose [16–18], choline [19,20], and thymidine [21]. On the basis of changes in uptake of these radiolabeled metabolites, PET imaging methods have been successful in both staging of diverse cancers and assessment of response of tumors to therapy [22–24].

Despite significant clinical success, it is widely recognized that PET imaging methods have limited spatial resolution [25]. In addition, PET imaging typically requires large radioisotope generation facilities at the imaging site due to short half-life (such as 110 minutes for ^{18}FDG PET tracer; 20 minutes for ^{11}C-Choline) of many commonly used radiolabeled tracers [25].

Development of optical molecular probes that can measure the same molecular events as detected using the current PET imaging methods can provide a complementary imaging approach. This complementary imaging approach cannot only address some of the limitations of PET imaging and but also enhance fundamental understanding of disease processes such as molecular changes in epithelial tissues during early stages of neoplasia. Indeed, the impact of combining PET or magnetic resonance (MR) imaging with optical molecular imaging (multimodality molecular imaging) has been successfully demonstrated in various studies in animal model systems [26–28].

With this motivation, a molecular analogue of choline with a monoalkyne modification (propargyl choline) was synthesized. This analogue of choline can be detected *in situ* using the click chemistry reaction with an azide-modified fluorophore. Choline is a small molecule metabolite that is an essential substrate for synthesis of phosphatidylcholine, a major component of cell membrane [29]. Radiolabeled choline analogues are being currently evaluated for clinical applications in cancer detection and therapy evaluation using PET imaging [30,31]. Application of choline analogues in cancer detection is based on an understanding that cancer cells have increased rates of uptake and intracellular phosphorylation of choline compared to normal epithelial cells [32,33]. The increased intracellular uptake and retention of choline in cancer cells has also been correlated with enhanced biochemical activity and expression of choline kinase enzymes and choline transporters, respectively [32,33].

The focus of this study was to develop an optical molecular imaging approach to measure differences in uptake and intracellular retention of choline in clinically isolated paired (clinically abnormal and normal tissues) fresh tissue biopsies from head and neck cancer patients. Head and neck cancer is an excellent target for developing and validating optical molecular imaging approaches as oral cavity is an easily accessible site for optical imaging. Head and neck cancer, like other epithelial-derived cancers, is initiated by molecular transformation of cells in epithelial tissue that can be imaged using optical imaging methods [34–37]. In addition, molecular contrast media can be locally applied to suspicious lesions within the oral cavity [38,39], thus, enabling a rapid and a noninvasive evaluation of local tissue with molecular-specific imaging approaches.

In summary, an optically detectable analogue of choline (propargyl choline) was synthesized and evaluated in 2D and 3D cell culture models and clinically isolated intact fresh paired biopsies from head and neck cancer patients. Topical application was used for delivery of propargyl choline in a 3D tissue model and clinically isolated fresh tissues. Following topical delivery of propargyl choline in intact fresh tissues, the tissues were transversely sectioned, *in situ* stained with an azide-modified dye, and imaged using confocal microscopy. Fluorescence contrast resulting from uptake of propargyl choline was quantified in the epithelial region of tissue sections. Results from imaging measurements were correlated with pathologic diagnosis of clinically isolated paired biopsies.

Materials and Methods

Cell Lines and Culture

The human cervical carcinoma cell line HeLa was maintained in a culture medium consisting of Dulbecco's modified Eagle's medium (Fisher Scientific, Pittsburgh, PA) supplemented with 10% FBS (Fisher Scientific) and 100 mg/l penicillin (Sigma, St Louis, MO). HeLa cells (4×10^4 cells/ml) were seeded into culture flasks, grown in a humidified atmosphere of 5% CO_2/95% air at 37°C, and subcultured with 0.05% trypsin (Invitrogen, Carlsbad, CA). For imaging, cells were cultured on eight-well coverslip bottom cell culture chambers (Fisher Scientific).

Tissue Phantoms

Tissue phantoms were prepared using HeLa cells embedded in a collagen matrix. Type I collagen (Roche, South San Francisco, CA) was dissolved in 0.2% acetic acid to a final concentration of 3 mg/ml. To prepare tissue phantoms, a suspension of HeLa cells was spun down and resuspended in a small volume of Dulbecco's modified Eagle's medium (Invitrogen) containing 5% FBS to achieve a final concentration of 1×10^8 cells per milliliter of media. Collagen and cells were mixed together (two parts of collagen were mixed with one part of media with cells) to form a suspension. NaOH (1 M) was gradually added to the suspension to achieve a final pH of 7.4. The suspension was gently transferred into 24-mm transwells with 3.0-μm pore polycarbonate membrane (Corning Incorporated, Corning, NY). These transwells were then placed in individual wells of a 24-well plate with media. Collagen-cell matrix formed a gel within 30 minutes of incubation at 37°C. After forming the gel, 40 μl of cell culture medium was added on top of the tissue phantom. Tissue phantoms were cultured for 48 hours to develop a dense cellular network in collagen gel that mimics both the structural features and the optical properties of oral epithelial tissues [40].

Synthesis of Propargyl Choline

Propargyl choline was synthesized on the basis of the procedure described by Jao et al. [41]. Four grams of propargyl bromide (80% solution in toluene) was added to 3 g of dimethylethanolamine in 10 ml of tetrahydrofuran. The mixture was gently stirred over ice for approximately 30 minutes. The reaction mixture was purged with nitrogen for 24 hours. Propargyl choline (white solid) was separated from the solvent by filtration (Millipore filter, 0.22 μm, Billerica, MA) followed by repeated washing with tetrahydrofuran. The final product was freeze dried and stored at −20°C.

Specificity of Detecting Propargyl Choline in Cell Culture Models

Cells were incubated with propargyl choline (2 mM propargyl choline was added to regular cell culture media) for 1 hour at 37°C. Control cell samples were incubated without propargyl choline. Both the treatment and the control samples were then washed with

phosphate-buffered saline (PBS) and fixed with 3.7% formaldehyde. After 30 minutes of fixation, formaldehyde solution was removed and the cells were washed three times with 1× PBS. Both propargyl choline labeled and control cells were incubated with the click chemistry reaction buffer for 30 minutes. Composition of the reaction buffer was 0.1 M Tris buffer (pH = 8.5) with 0.05% Triton, 10 μM Alexa 488 azide, 1 mM $CuSO_4$, and 50 mM ascorbic acid. After 30 minutes of incubation, cells were washed with PBS and imaged using an inverted fluorescence microscope (IX71 Olympus Inc, Center Valley, PA). Excitation and emission filters for fluorescence microscopy were 470 ± 15 and 515 to 550 nm, respectively. Exposure time for the charge-coupled device (CCD) camera was 500 ms. Fluorescence images were acquired by MetaMorph image analysis software (Olympus Inc).

Competition Assay

A competition assay was designed to demonstrate specificity of uptake of propargyl choline through choline transporters. HeLa cells were co-incubated with a fixed concentration of propargyl choline (2 mM) and a varying concentration of unmodified choline (ranging from 0 to 60 mM), respectively. After co-incubation of cells with a mixture of propargyl choline and choline for 1 hour, cells were fixed, stained, and imaged using the procedure described in the previous section.

Specificity of Propargyl Choline Uptake in 3D Tissue Phantom Model

To image uptake and intracellular retention of choline in epithelial tissues, propargyl choline was topically delivered in 3D tissue phantoms and clinically isolated biopsies (60 minutes of incubation). Following topical delivery, tissue phantoms were rinsed and transversely sectioned (approximately 200-μm-thick slices) using an oscillating tissue slicer (EMS 5000, Electron Microscopy Sciences Inc, Hatfield, PA). Individual slices were fixed using 3.7% formaldehyde in PBS at 4°C. After 30 minutes of fixation, formaldehyde was removed and the specimens were washed three times with 1× PBS. The sliced samples were incubated with the click chemistry reaction buffer as described in the previous section. Spatial distribution of propargyl choline within a tissue section was measured using confocal fluorescence microscopy (Zeiss LSM 510) with a 488-nm laser excitation filter and a 500- to 550-nm band-pass emission filter.

Collection of Biopsies

Pairs of clinically normal and abnormal biopsies were obtained from consenting patients who were scheduled for diagnostic mapping biopsies or surgical removal of an upper aerodigestive tract tumor. Each patient provided one clinically normal appearing biopsy and one or two clinically abnormal appearing biopsies (2 mm to 6 mm in diameter). The paired biopsy samples were kept fresh in cold normal saline (0.9% NaCl) and were transported to the laboratory in less than 30 minutes.

Topical Labeling of Intact Biopsies

Clinically isolated fresh tissue biopsies were labeled with propargyl choline using a topical application. For topical delivery, saline solution containing 2 mM propargyl choline and 10% DMSO was applied on the mucosal surface of clinically isolated intact biopsies. The details of topical delivery of contrast media in isolated biopsies and resected tumors are described in our previous studies [42]. After 60 minutes of incubation at 37°C, the biopsies were washed in normal saline for 10 minutes to remove any unbound propargyl choline.

Tissue Sectioning and Staining

Fresh tissue biopsies after topical delivery of propargyl choline were transversely sectioned using an oscillating tissue slicer (EMS 5000) to obtain 150- to 200-μm-thick fresh tissue slices. Tissue slices were fixed, stained with Alexa 555 azide, and washed with PBS using the same protocol as described earlier. Fluorescence and white light [differential interference contrast (DIC)] images of transverse sections of tissues were acquired using a laser scanning confocal fluorescence microscope (Zeiss LSM 510) with a 543-nm laser excitation and a 535- to 590-nm emission filter.

Quantification of Imaging Data

To quantify imaging measurements in 2D cells, mean fluorescence intensity (MFI) of individual cells within the field of view (FOV) was calculated using ImageJ (Public domain, National Institutes of Health). The MFI of individual cells was quantified by subtracting the background fluorescence intensity calculated from a region on a chamber coverslip without any cells. It is important to note that fluorescence intensity corresponding to background fluorescence and cellular autofluorescence was significantly small compared to the fluorescence signal from stained cells. Multiple FOVs (typically 9–10 FOVs with approximately 90–120 cells in total) were analyzed to calculate the MFI from three independent repeat experiments for each of the experimental conditions. Average MFI and SD were calculated for each of the experimental conditions. The MFI of transverse sections of 3D phantoms was also calculated using ImageJ.

High-resolution fluorescence images of the isolated biopsy slices were analyzed to quantify the MFI of clinically abnormal samples and clinically normal samples. For quantification of the MFI, epithelial region within the tissue section was identified on the basis of DIC image of the transverse tissue section. The selected region identified in the DIC image was overlaid on the corresponding fluorescence image and the MFI of the selected region was calculated using ImageJ. Similar approach was used in our prior studies to quantify the MFI within the epithelial region of labeled fresh tissue sections [42]. Fluorescence contrast ratio was calculated on the basis of the ratio of average MFIs of clinically abnormal and normal biopsy samples. For calculating the average MFI, three individual images per biopsy sample were acquired and analyzed as described above. The quantified imaging results were statistically analyzed using analysis of variance.

Pathologic Diagnosis

Following imaging, fixed tissue sections were embedded in paraffin and submitted for hematoxylin and eosin staining and examined by Dr. Gandour-Edwards, a board-certified pathologist at the University of California, Davis. The results from fluorescence imaging measurements were correlated with the pathologic diagnosis.

Results

Chemical Structure of Propargyl Choline and In Situ *Labeling of Propargyl Choline in Cells*

Figure 1 shows the schematic overview of intracellular uptake and *in situ* labeling of propargyl choline using the click chemistry reaction.

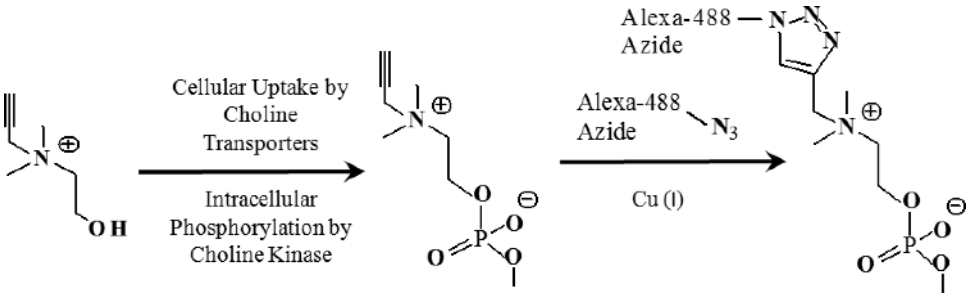

Figure 1. Pathway for cellular uptake and intracellular retention of propargyl choline. Intracellular retained propargyl choline can be imaged using the click chemistry reaction with an azide-modified fluorophore.

Propargyl choline is an analogue of choline with a monoalkyne tag at its N terminus. Intracellular uptake of propargyl choline can be detected on the basis of *in situ* labeling of propargyl choline with an azide-modified fluorophore as illustrated in Figure 1.

Imaging Uptake of Propargyl Choline in 2D Cell Culture and 3D Tissue Phantom Models

Results in Figure 2*A* demonstrate a rapid uptake (approximately 60 minutes of incubation) of propargyl choline by HeLa cells. Fluorescent signal based on *in situ* labeling of propargyl choline was predominantly localized in the cytoplasm of individual cells. Prior studies have shown that choline molecules are phosphorylated in the cytoplasm of cells by choline kinase enzymes [43,44]. In comparison to the results in Figure 2*A*, the negative control cells (not incubated with propargyl choline but stained with Alexa 488 azide dye) show no significant fluorescent labeling (Figure 2*B*).

Results in Figure 2*C* illustrate that topical delivery was sufficient to achieve uniform permeation of propargyl choline across the thickness of tissue phantoms (approximately 1-mm thickness) within 60 minutes of incubation. To characterize permeation of propargyl choline in tissue phantoms, transverse sections of tissue phantoms were evaluated. Fluorescence contrast in transverse tissue sections was predominantly localized in the cytoplasm of cells and no significant retention and/or binding of propargyl choline with the extracellular matrix was observed. This observation demonstrates that simple rinsing of intact tissue phantoms with PBS buffer was sufficient to remove excess propargyl choline from the extracellular matrix of tissue phantoms. Results of control experiments (tissue phantoms stained with Alexa 488 azide without any prior incubation with propargyl choline) demonstrate lack of nonspecific staining of Alexa 488 azide in tissue phantoms. Together, these results demonstrate a rapid intracellular uptake of propargyl choline, high specificity of the click chemistry staining reaction in cells and tissue phantoms, and a uniform permeation of topical delivered propargyl choline in tissue phantoms.

Competition Assay to Evaluate Specificity of Uptake of Propargyl Choline

To evaluate specificity of propargyl choline uptake, a competition assay was designed by varying the concentration of choline chloride in cell culture medium with a fixed concentration of propargyl choline. Results in Figure 3*A* show a progressive decrease in fluorescent staining of cells (resulting from decreased uptake of propargyl choline) as the concentration of choline chloride (0–60 mM) was increased in the extracellular environment. The results show that even a low concentration of choline chloride (0.2 mM, approximately 10-fold lower than the concentration level of propargyl choline in media) was sufficient to reduce uptake of propargyl choline. At concentration levels in the range of 20 to 60 mM choline chloride (10-fold to 30-fold higher than the concentration of propargyl choline), no detectable fluorescent signal in cells incubated with propargyl choline was observed. Figure 3*B* compares the relative MFI in individual cells as the concentration of choline chloride was increased in the cell culture medium. These results show that competition between propargyl choline and choline chloride resulted in a significant decrease in uptake of propargyl choline.

Imaging Uptake of Propargyl Choline in Clinically Normal and Abnormal Head and Neck Biopsies Following Topical Delivery

Table 1 shows the diverse anatomic locations within the head and neck cavity from which the paired biopsies were isolated and the corresponding pathologic diagnosis. Nine consenting patients at UC Davis Medical Center (UCDMC) provided 9 clinically normal biopsies and 13 distinct clinically abnormal biopsies. When multiple abnormal biopsies were obtained, they were collected from the same anatomic region (e.g., both were from the base of tongue) but distinct locations within the tumor. Although paired set of biopsies were obtained from a variety of anatomic locations, there was a predominance of tonsillar tissue including both palatine tonsils and the base of tongue (81% of abnormal biopsies and 66% of normal biopsies). This reflects the current population of patients seen in the otolaryngology clinic. Nine of the clinically abnormal appearing samples were diagnosed as invasive squamous cell carcinoma (SCC), which reflects the current clinical trend that the head and neck cancers are often detected and treated at late stages of the disease. Two biopsies were diagnosed as carcinoma *in situ* (CIS). Despite appearing abnormal clinically, two biopsies were diagnosed as normal based on the pathology review. The clinical surgical pathology report concurred with the pathologic findings of these biopsies. Patients ranged from 51 to 84 years old, and 75% were male. All of the patients had no prior history of oropharyngeal carcinoma.

The freshly excised tissue biopsies were labeled using topical delivery of propargyl choline. Transverse tissue sections of the labeled biopsies were imaged as described in the Materials and Methods section. The resulting fluorescence contrast was compared between clinically abnormal and normal biopsies. Figure 4*A* shows a representative data for a paired biopsy set (paired clinically abnormal and normal) isolated from an individual patient. The data set shows fluorescence imaging measurements of transverse tissue sections of both clinically abnormal

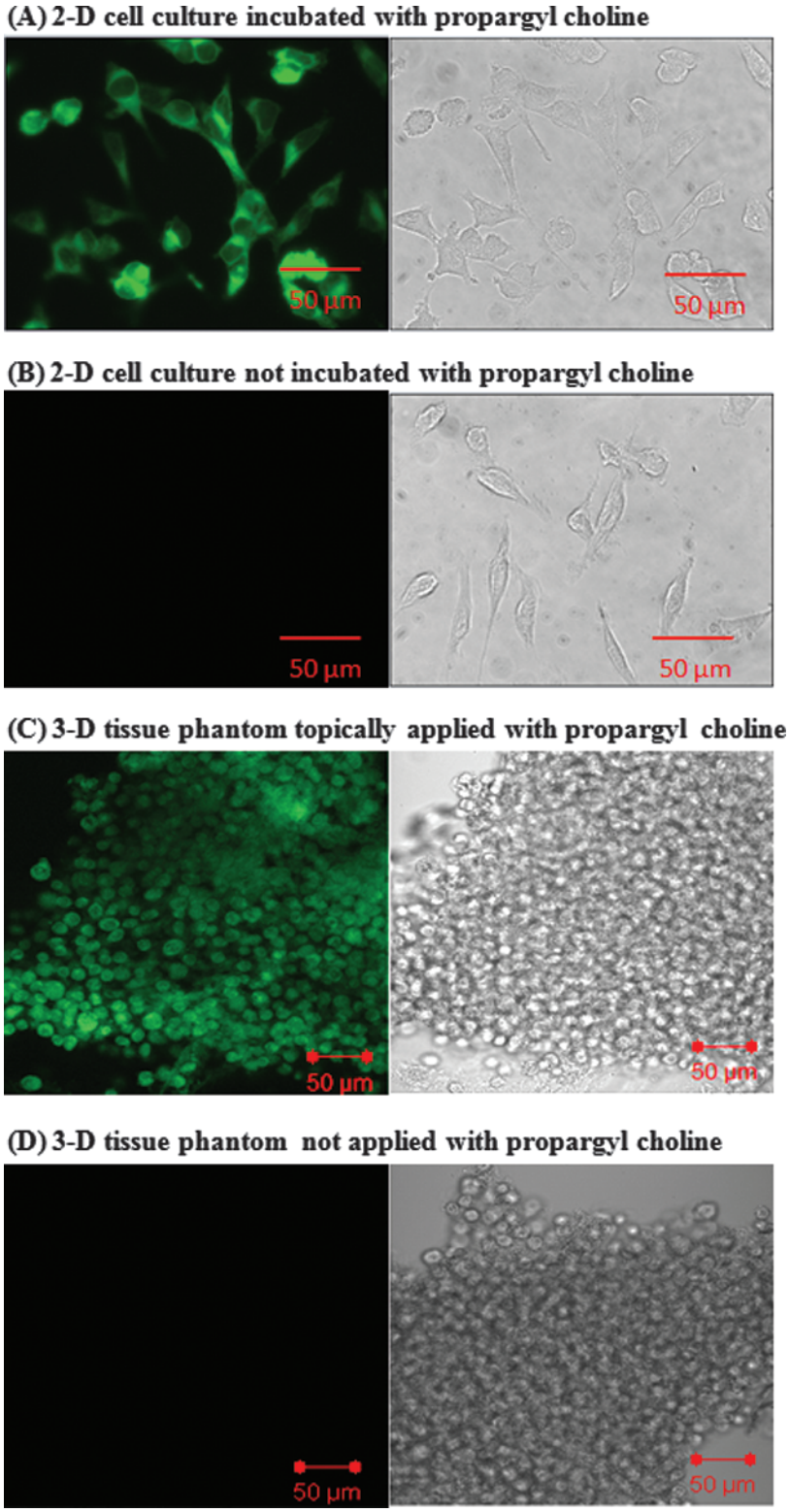

Figure 2. Imaging uptake of propargyl choline in 2D cell culture and 3D tissue phantom models. Fluorescence and corresponding white light images of HeLa cells incubated (A) with propargyl choline for 1 hour and stained with Alexa 488 azide and (B) without propargyl choline but stained with Alexa 488 azide. (C) Propargyl choline was topically delivered in 3D tissue phantom. Fluorescence and corresponding white light images of transverse section of tissue phantoms were acquired after fixation and staining with Alexa 488 azide. (D) Control tissue phantom was not incubated with propargyl choline but was sliced, fixed, and stained with Alexa 488 azide.

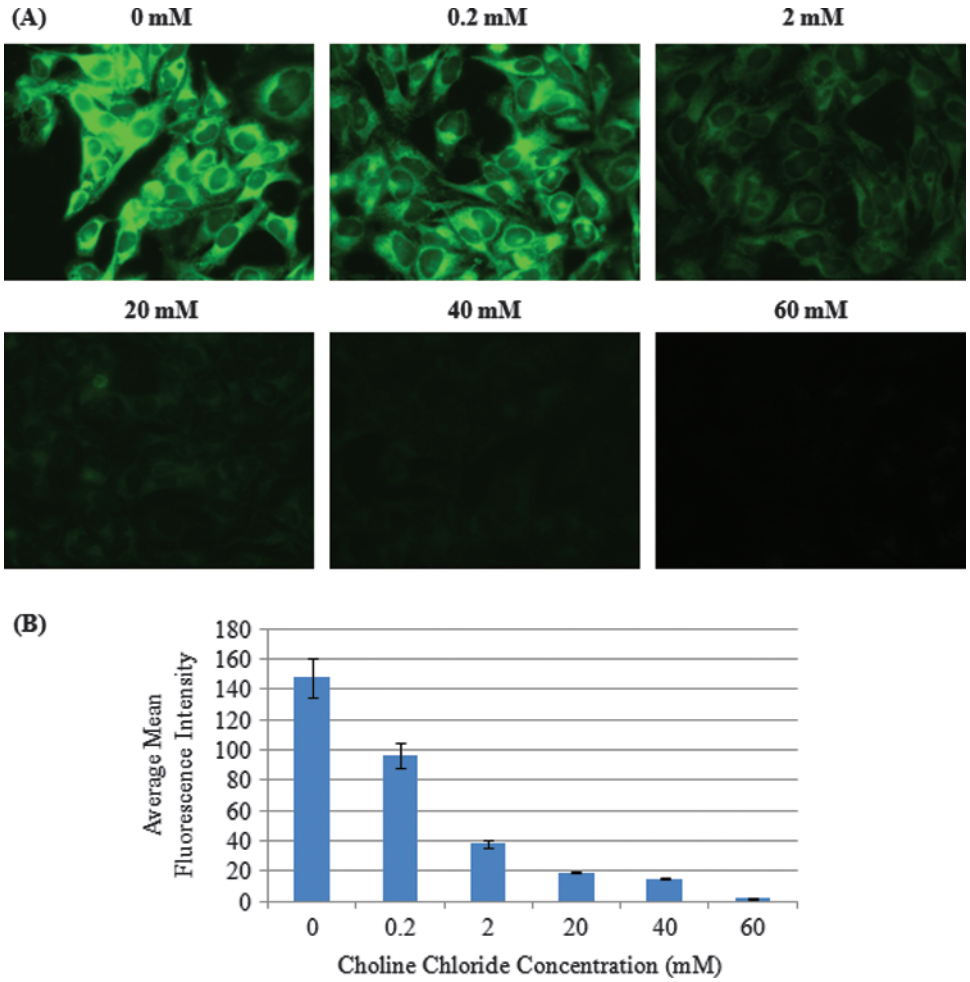

Figure 3. (A) Competition assay to characterize specificity of uptake of propargyl choline in cells. HeLa cells were co-incubated with a fixed concentration (2 mM) of propargyl choline and increasing concentration of choline chlorine (0–60 mM). After incubation, the cells were fixed and stained with Alexa 488 azide. (B) Decrease in MFI (corresponding to uptake of propargyl choline) as a function of increasing concentration of choline chloride in cell culture media.

and normal biopsies and their corresponding hematoxylin and eosin slides with pathologic diagnosis. In this particular paired biopsy set, the abnormal biopsy was diagnosed as invasive SCC, whereas the paired clinical normal biopsy was diagnosed as normal based on histologic analysis. In the cancer biopsy, significant fluorescent staining corresponding to enhanced uptake and intracellular retention of propargyl choline by cancer cells was detected. In the normal biopsy, negligible fluorescence staining with propargyl choline was observed. Thus, significant differences in fluorescence contrast can be measured between clinically abnormal and normal biopsies. Figure 4*B* shows comparison between a set of biopsies in which the clinically abnormal biopsy was diagnosed as normal based on pathologic review. In contrast to the results in Figure 4*A*, this clinically abnormal but pathologically normal sample had similar fluorescence staining compared to the paired normal biopsy. In both the clinically abnormal and normal samples, faint fluorescent staining was observed throughout the epithelial section of the tissue.

Table 1. Clinically Isolated Paired Biopsies and Their Pathologic Diagnosis.

Patient No.	Clinically "Abnormal" Location	Pathologic Diagnosis	Clinically "Normal" Location	Pathologic Diagnosis
1	Tonsil	Invasive SCC	Tonsil	Normal
2 A and B	Tonsil	Invasive SCC	Tonsil	Normal
3 A and B	Tonsil	Invasive SCC	Tonsil	Normal
4	Tonsil	Invasive SCC	Base of tongue	Normal
5 A and B	Base of tongue	CIS	Base of tongue	Normal
6 A and B	Base of tongue	Normal	Base of tongue	Normal
7	Floor of mouth	Invasive SCC	Buccal	Normal
8	Hard palate	Invasive SCC	Buccal	Normal
9	Larynx	Invasive SCC	Epiglottis	Normal

Comparison of Fluorescence Contrast between Clinically Abnormal and Clinical Paired Biopsy Sets as a Function of Pathologic Diagnosis

Figure 5*A* shows the relative fluorescence contrast ratio (ratiometric contrast) of paired biopsies separated by pathologic diagnosis. The MFI for cancer biopsies (n = 9 paired biopsies) was four-fold to five-fold higher than the MFI of paired normal biopsies. In this study, there were two paired biopsy sets that were diagnosed as CIS (n = 2). The MFI for the CIS biopsies was 3.5-fold higher than the MFI of paired normal biopsies. For the pathologically normal biopsies (initially identified as clinically abnormal biopsies, n = 2), the MFI was similar to the MFI of paired normal biopsies. As a result, the ratiometric contrast ratio of 1 to 1.5 was calculated for these sets of biopsies. This result demonstrates specificity of propargyl choline–based imaging approach to distinguish true pathologically cancer biopsy from normal biopsies. It is important to note that many head and cancer patients are diagnosed at late stages of the disease, so the percentage of patients detected at early stages of cancer (CIS and dysplasia) are significantly small and it is rare to have a clinically abnormal biopsy that is diagnosed as normal in a pathologic review. As a result of these clinical aspects, the number of biopsies for the CIS and normal are small for developing a statistically significant comparison.

To demonstrate potential of this imaging approach to distinguish clinically abnormal tissues from normal tissues across diverse patients, high-resolution imaging results were compared independent of the paired biopsy sets and anatomic locations within the head and neck cavity. Figure 5*B* shows the unpaired comparison between all cancerous and normal biopsies, irrespective of anatomic location within the head and neck cavity. The results show that the MFI in cancer

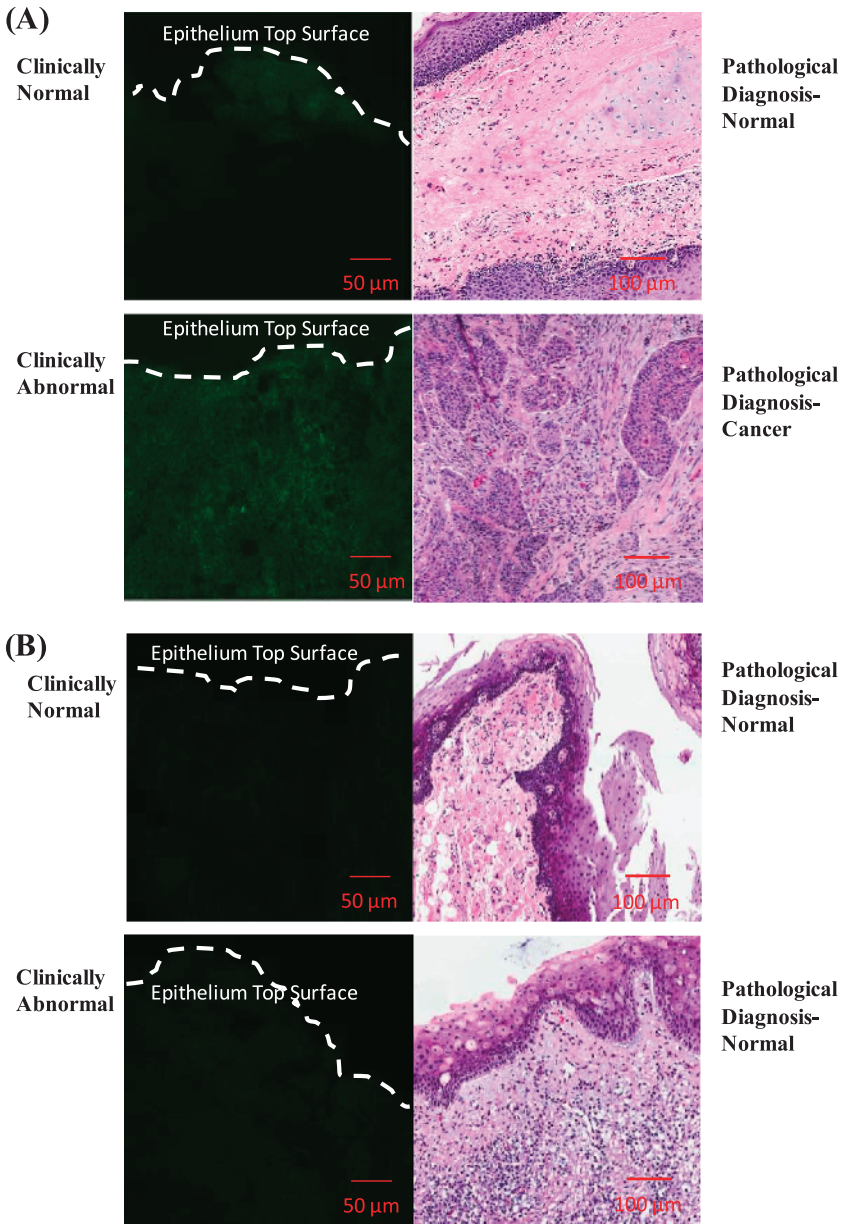

Figure 4. Confocal fluorescence images (left) and corresponding pathologic diagnosis (right) of paired oral biopsy specimens topically labeled with propargyl choline. Two representative cases of paired sets of biopsies are shown. (A) The pathologic diagnosis of the clinically abnormal biopsy was invasive SCC, whereas the paired normal biopsy was diagnosed as normal. (B) The pathologic diagnosis of the clinically abnormal biopsy was normal, whereas the diagnosis of the clinically normal biopsy was normal.

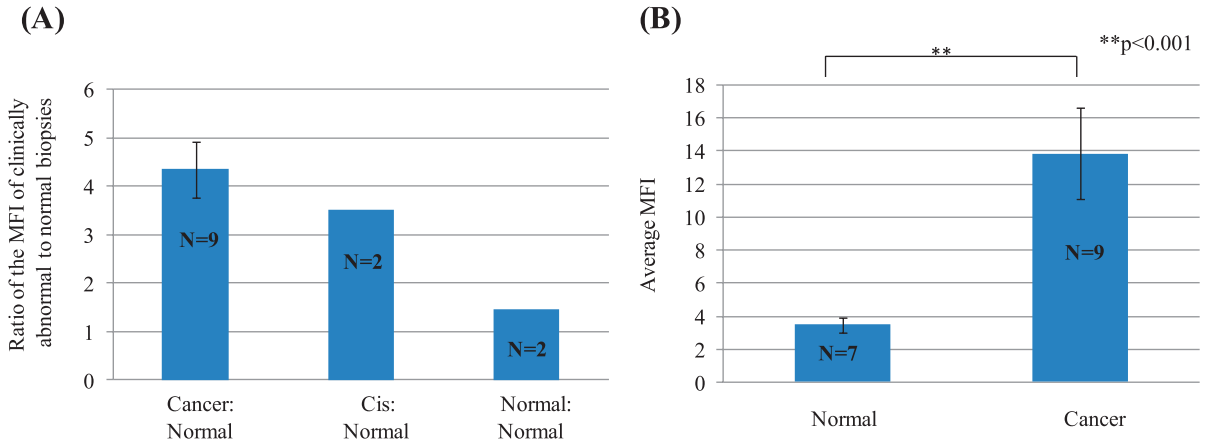

Figure 5. (A) Ratiometric contrast measurement to compare the ratio of MFI resulting from uptake of propargyl choline in paired sets of biopsies from individual patients. Results are plotted as a function of pathologic diagnosis. (B) Comparison of fluorescence contrast in clinically isolated biopsies across multiple patients and diverse anatomic sites in oral cavity. Average fluorescence signal intensity in clinically and histologically diagnosed normal ($n = 8$) and cancerous ($n = 11$) oral biopsy specimens labeled with propargyl choline was quantified (**$P < .001$).

biopsies is four to five times higher than the MFI of normal biopsies. These results clearly demonstrate that cancerous tissues have a significantly higher uptake and intracellular retention of propargyl choline compared to normal tissues and that this difference can be discriminated even when averaged over a heterogeneous sampling of anatomic locations and patients.

Discussion

In this study, a monoalkyne analogue of choline (propargyl choline) was synthesized for imaging uptake and intracellular retention of choline in cell culture models and clinically isolated fresh tissues. Using this nonfluorescent analogue of choline as a metabolic tracer, uptake of propargyl choline was imaged on the basis of the click chemistry reaction between an intracellular entrapped monoalkyne choline and an azide-linked fluorophore. Monoalkyne modification of choline does not significantly increase the molecular weight and the size of native choline molecule. This is a critical factor as previous studies [45] have shown that direct conjugation of fluorescent dyes with small molecules can significantly influence specificity of intracellular uptake of metabolites. One of the potential limitations of the current approach is that the detection process involves a two-step labeling procedure. In the first step, cells were incubated with propargyl choline, and in the following step, labeled cells were reacted with an azide-functionalized fluorescent dye in the presence of copper ions. Currently, significant research efforts are being made to develop copper-free click chemistry probes for intracellular imaging [46,47]. These developments combined with optical imaging technologies such as fiber optic confocal systems will enable translation of these measurements to *in vivo* imaging in a clinical environment [48].

The results of this study demonstrate delivery of propargyl choline in oral epithelium using topical application. These results are in agreement with our previous study in which we have demonstrated efficient topical delivery of fluorescently labeled deoxyglucose molecule in clinically isolated biopsies and resected tumor tissues [42]. Topical delivery of contrast media is a common approach used in many clinical diagnostic evaluations and has significant advantages compared to the commonly used intravenous injection [49]. Topical delivery provides a rapid access to the target epithelial tissue. Using intravenous approach, delivery and distribution of contrast agents is controlled by blood circulation. Lack of vasculature in the epithelial layer on early stages of neoplasia can limit delivery of contrast media to the target tissue. Furthermore, topical delivery significantly reduces nonspecific interaction of molecular imaging probes with nontargeted tissues. Therefore, it reduces the amount of contrast agent and the time required for imaging. On the basis of the results of this study and our prior studies [42], we have demonstrated that excess or unbound contrast media can be easily removed from intact tissue biopsies by simply rinsing the tissue with excess buffer.

High-resolution imaging results demonstrate a significant increase in fluorescence contrast in clinically abnormal samples compared to normal samples. In the cohort of samples ($n = 22$ biopsies), the fluorescence contrast was approximately four-fold to five-fold higher in clinically and pathologically abnormal cancer biopsies compared to normal biopsies. In addition to detecting differences between cancer and normal biopsies, the molecular imaging approach had high specificity in identifying normal tissue that was considered clinically abnormal based on the clinical impression. In these paired biopsies, the clinically abnormal appearing tissue (but pathologically normal) biopsy did not show a significant increase in fluorescence contrast compared to the paired clinically and pathologically normal tissues. This result highlights specificity of differentiating between true clinical abnormal and normal tissues.

In summary, the results of this study have demonstrated that topically applied propargyl choline has significant potential to differentiate cancerous tissues from surrounding normal tissues in a variety of anatomic locations across a diverse group of patients.

Conclusion

The study demonstrates development and validation of a novel optical imaging approach and its translation using clinically isolated fresh tissue samples. Changes in uptake and intracellular retention of choline in clinically isolated head and neck biopsies were measured using a novel optical imaging approach. Optical molecular imaging results were compared with pathologic diagnosis of these biopsies. The results show that propargyl choline can be rapidly delivered to oral epithelium using topical application. The results of this study demonstrate that optical imaging of changes in choline uptake and intracellular retention can

distinguish between clinically normal and abnormal biopsies. Results of imaging measurements are in agreement with pathologic diagnosis. Overall, these results demonstrate clinical potential of the molecular imaging approach and its application in improving detection and prognostic evaluation of head and neck cancer.

References

[1] Sokolov K, Aaron J, Hsu B, Nida D, Gillenwater A, Follen M, MacAulay C, Adler-Storthz K, Korgel B, Descour M, et al. (2003). Optical systems for *in vivo* molecular imaging of cancer. *Technol Cancer Res Treat* **2**, 491–504.

[2] Choy G, Choyke P, and Libutti SK (2003). Current advances in molecular imaging: noninvasive *in vivo* bioluminescent and fluorescent optical imaging in cancer research. *Mol Imaging* **2**, 303–312.

[3] Weissleder R (2006). Molecular imaging in cancer. *Science* **312**, 1168–1171.

[4] Thekkek N and Richards-Kortum R (2008). Optical imaging for cervical cancer detection: solutions for a continuing global problem. *Nat Rev Cancer* **8**, 725–731.

[5] Luker GD and Luker KE (2008). Optical imaging: current applications and future directions. *J Nucl Med* **49**, 1–4.

[6] Blasberg RG (2003). Molecular imaging and cancer. *Mol Cancer Ther* **2**, 335–343.

[7] Vila PM, Thekkek N, Richards-Kortum R, and Anandasabapathy S (2011). Use of *in vivo* real-time optical imaging for esophageal neoplasia. *Mt Sinai J Med* **78**, 894–904.

[8] Kumar S and Richards-Kortum R (2006). Optical molecular imaging agents for cancer diagnostics and therapeutics. *Nanomedicine (Lond)* **1**, 23–30.

[9] Pierce MC, Javier DJ, and Richards-Kortum R (2008). Optical contrast agents and imaging systems for detection and diagnosis of cancer. *Int J Cancer* **123**, 1979–1990.

[10] Pierce M, Nitin N, Mayes W, Javier D, Follen M, Gillenwater A, and Richards-Kortum R (2007). *In vivo* confocal microscopy and optical contrast agents. *Acta Cytol* **51**, 265.

[11] Jaffer FA and Weissleder R (2005). Molecular imaging in the clinical arena. *JAMA* **293**, 855–862.

[12] Blasberg RG (2003). *In vivo* molecular-genetic imaging: multi-modality nuclear and optical combinations. *Nucl Med Biol* **30**, 879–888.

[13] Thekkek N, Maru DM, Polydorides AD, Bhutani MS, Anandasabapathy S, and Richards-Kortum R (2011). Pre-clinical evaluation of fluorescent deoxyglucose as a topical contrast agent for the detection of Barrett's-associated neoplasia during confocal imaging. *Technol Cancer Res Treat* **10**, 431–441.

[14] Thekkek N, Anandasabapathy S, Maru D, and Richards-Kortum R (2009). Using a fluorescently labeled glucose analog as an optical biomarker for the early detection of cancer in Barrett's esophagus. *Gastroenterology* **136**, A647.

[15] Sevick-Muraca EM (2012). Translation of near-infrared fluorescence imaging technologies: emerging clinical applications. *Annu Rev Med* **63**, 217–231.

[16] Gambhir SS (2002). Molecular imaging of cancer with positron emission tomography. *Nat Rev Cancer* **2**, 683–693.

[17] Czernin J and Phelps ME (2002). Positron emission tomography scanning: current and future applications. *Annu Rev Med* **53**, 89–112.

[18] Czernin J (2002). Clinical applications of FDG-PET in oncology. *Acta Med Austriaca* **29**, 162–170.

[19] Khan N, Oriuchi N, Ninomiya H, Higuchi T, Kamada H, and Endo K (2004). Positron emission tomographic imaging with 11C-choline in differential diagnosis of head and neck tumors: comparison with 18F-FDG PET. *Ann Nucl Med* **18**, 409–417.

[20] Rinnab L, Mottaghy FM, Blumstein NM, Reske SN, Hautmann RE, Hohl K, Moller P, Wiegel T, Kuefer R, and Gschwend JE (2007). Evaluation of [^{11}C]-choline positron-emission/computed tomography in patients with increasing prostate-specific antigen levels after primary treatment for prostate cancer. *BJU Int* **100**, 786–793.

[21] Buck AK, Herrmann K, Shen C, Dechow T, Schwaiger M, and Wester HJ (2009). Molecular imaging of proliferation *in vivo*: positron emission tomography with [^{18}F]fluorothymidine. *Methods* **48**, 205–215.

[22] Rohren EM, Turkington TG, and Coleman RE (2004). Clinical applications of PET in oncology. *Radiology* **231**, 305–332.

[23] Wiseman GA, Juweid ME, Rohren EM, Wooldridge JE, and Graham MM (2004). FDG PET scan alone better predicts progression free survival at 2 years compared to CT imaging in aggressive histology non-Hodgkin's lymphoma following initial anthracycline-based chemotherapy. *Blood* **104**, 901a.

[24] Arens AIJ, Troost EGC, Schinagl D, Kaanders JHAM, and Oyen WJG (2011). FDG-PET/CT in radiation treatment planning of head and neck squamous cell carcinoma. *Q J Nucl Med Mol Imaging* **55**, 521–528.

[25] Blodgett TM, Meltzer CC, and Townsend DW (2007). PET/CT: form and function. *Radiology* **242**, 360–385.

[26] Culver J, Akers W, and Achilefu S (2008). Multimodality molecular imaging with combined optical and SPECT/PET modalities. *J Nucl Med* **49**, 169–172.

[27] Ray P, Wu AM, and Gambhir SS (2003). Optical bioluminescence and positron emission tomography imaging of a novel fusion reporter gene in tumor xenografts of living mice. *Cancer Res* **63**, 1160–1165.

[28] Gulsen G, Birgul O, Unlu MB, Shafiiha R, and Nalcioglu O (2006). Combined diffuse optical tomography (DOT) and MRI system for cancer imaging in small animals. *Technol Cancer Res Treat* **5**, 351–363.

[29] Vance JE and Vance DE (2004). Phospholipid biosynthesis in mammalian cells. *Biochem Cell Biol* **82**, 113–128.

[30] de Jong IJ, Pruim J, Elsinga PH, Vaalburg W, and Mensink HJ (2003). ^{11}C-choline positron emission tomography for the evaluation after treatment of localized prostate cancer. *Eur Urol* **44**, 32–38; discussion 38–39.

[31] Breeuwsma AJ, Pruim J, van den Bergh ACM, Leliveld AM, Njman RJM, Dierckx RAJO, and de Jong IJ (2010). Detection of local, regional, and distant recurrence in patients with Psa relapse after external-beam radiotherapy using ^{11}C-choline positron emission tomography. *Int J Radiat Oncol Biol Phys* **77**, 160–164.

[32] de Molina AR, Rodriguez-Gonzalez A, Gutierrez R, Martinez-Pineiro L, Sanchez JJ, Bonilla F, Rosell R, and Lacal JC (2002). Overexpression of choline kinase is a frequent feature in human tumor-derived cell lines and in lung, prostate, and colorectal human cancers. *Biochem Biophys Res Commun* **296**, 580–583.

[33] de Molina AR, Gutierrez R, Ramos MA, Silva JM, Silva J, Bonilla F, Sanchez JJ, and Lacal JC (2002). Increased choline kinase activity in human breast carcinomas: clinical evidence for a potential novel antitumor strategy. *Oncogene* **21**, 4317–4322.

[34] Roblyer D, Richards-Kortum R, Sokolov K, El-Naggar AK, Williams MD, Kurachi C, and Gillenwater AM (2008). Multispectral optical imaging device for *in vivo* detection of oral neoplasia. *J Biomed Opt* **13**, 024019.

[35] Muto M, Minashi K, Yano T, Saito Y, Oda I, Nonaka S, Omori T, Sugiura H, Goda K, Kaise M, et al. (2010). Early detection of superficial squamous cell carcinoma in the head and neck region and esophagus by narrow band imaging: a multicenter randomized controlled trial. *J Clin Oncol* **28**, 1566–1572.

[36] Lippert AR, Keshari KR, Kurhanewicz J, and Chang CJ (2011). A hydrogen peroxide-responsive hyperpolarized ^{13}C MRI contrast agent. *J Am Chem Soc* **133**, 3776–3779.

[37] Jo JA, Applegate BE, Park J, Shrestha S, Pande P, Gimenez-Conti IB, and Brandon JL (2010). *In vivo* simultaneous morphological and biochemical optical imaging of oral epithelial cancer. *IEEE Trans Biomed Eng* **57**, 2596–2599.

[38] Lieb S, Szeimies RM, and Lee G (2002). Self-adhesive thin films for topical delivery of 5-aminolevulinic acid. *Eur J Pharm Biopharm* **53**, 99–106.

[39] Zhang L, Williams M, Poh CF, Laronde D, Epstein JB, Durham S, Nakamura H, Berean K, Hovan A, Le ND, et al. (2005). Toluidine blue staining identifies high-risk primary oral premalignant lesions with poor outcome. *Cancer Res* **65**, 8017–8021.

[40] Sokolov K, Galvan J, Myakov A, Lacy A, Lotan R, and Richards-Kortum R (2002). Realistic three-dimensional epithelial tissue phantoms for biomedical optics. *J Biomed Opt* **7**, 148–156.

[41] Jao CY, Roth M, Welti R, and Salic A (2009). Metabolic labeling and direct imaging of choline phospholipids *in vivo*. *Proc Natl Acad Sci USA* **106**, 15332–15337.

[42] Nitin N, Carlson AL, Muldoon T, El-Naggar AK, Gillenwater A, and Richards-Kortum R (2009). Molecular imaging of glucose uptake in oral neoplasia following topical application of fluorescently labeled deoxy-glucose. *Int J Cancer* **124**, 2634–2642.

[43] Ackerstaff E, Glunde K, and Bhujwalla ZM (2003). Choline phospholipid metabolism: a target in cancer cells? *J Cell Biochem* **90**, 525–533.

[44] Glunde K, Jacobs MA, and Bhujwalla ZM (2006). Choline metabolism in cancer: implications for diagnosis and therapy. *Expert Rev Mol Diagn* **6**, 821–829.

[45] Cheng Z, Levi J, Xiong ZM, Gheysens O, Keren S, Chen XY, and Gambhir SS (2006). Near-infrared fluorescent deoxyglucose analogue for tumor optical imaging in cell culture and living mice. *Bioconjug Chem* **17**, 662–669.

[46] Baskin JM, Prescher JA, Laughlin ST, Agard NJ, Chang PV, Miller IA, Lo A, Codelli JA, and Bertozzi CR (2007). Copper-free click chemistry for dynamic *in vivo* imaging. *Proc Natl Acad Sci USA* **104**, 16793–16797.

[47] Chang PV, Prescher JA, Sletten EM, Baskin JM, Miller IA, Agard NJ, Lo A, and Bertozzi CR (2010). Copper-free click chemistry in living animals. *Proc Natl Acad Sci USA* **107**, 1821–1826.

[48] Flusberg BA, Cocker ED, Piyawattanametha W, Jung JC, Cheung ELM, and Schnitzer MJ (2005). Fiber-optic fluorescence imaging. *Nat Methods* **2**, 941–950.

[49] Manganaro AM (1997). Review of the transmucosal drug delivery. *Mil Med* **162**, 27–30.